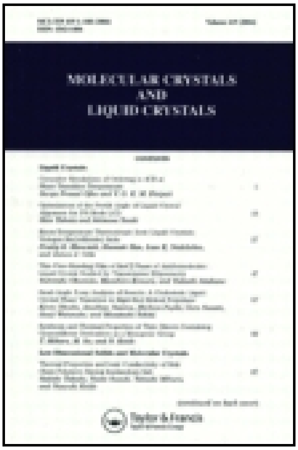

Molecular Crystals and Liquid Crystals Science and Technology. Section A. Molecular Crystals and Liquid Crystals

Publication details, including instructions for authors and subscription information:
http://www.tandfonline.com/loi/gmcl19

An Extended Peierls-Hubbard Model of Halogenbridged Transition Metal Chain Complexes

A. R. Bishop [a] , I. Batistić [a] , J. Tinka Gammel [a] & A. Saxena [a]

[a] Los Alamos National Laboratory, Los Alamos, New Mexico, 87545

Version of record first published: 04 Oct 2006.

To cite this article: A. R. Bishop , I. Batistić , J. Tinka Gammel & A. Saxena (1992): An Extended Peierls-Hubbard Model of Halogenbridged Transition Metal Chain Complexes, Molecular Crystals and Liquid Crystals Science and Technology. Section A. Molecular Crystals and Liquid Crystals, 218:1, 241-245

To link to this article: http://dx.doi.org/10.1080/10587259208047047

Mol. Cryst. Liq. Cryst. 1992, Vol. 218, pp. 241–245
Reprints available directly from the publisher
Photocopying permitted by license only

Printed in the United States of America

AN EXTENDED PEIERLS-HUBBARD MODEL OF HALOGEN-BRIDGED TRANSITION METAL CHAIN COMPLEXES

A. R. BISHOP, I. BATISTIĆ, J. TINKA GAMMEL, A. SAXENA
Los Alamos National Laboratory, Los Alamos, New Mexico 87545

Model calculations are described for both pure (MX) and mixed-halide ($MX_xX'_{1-x}$) halogen (X)-bridged transition metal (M) linear chain complexes in terms of an extended Peierls-Hubbard, tight-binding Hamiltonian with 3/4-filling of *two*-bands. Both inter- and intra-site electron-phonon coupling are included as well as various electron correlations. Calculated properties include electronic (optical absorption), lattice dynamic (IR, Raman) and spin (ESR) signatures for the ground states, localized excited states produced by impurities, doping or photoexcitation—excitons, polarons, bipolarons, solitons; and the edge states (which occur in mixed-halide crystals, e.g. $PtCl_xBr_{1-x}$). Adiabatic molecular dynamics is used to explore photodecay channels.

Halogen-bridged transition metal complexes (or MX chains), as well as being important in their own right, provide an important test case for theoretical techniques and issues in low-dimensional materials with strong electron-electron and electron-phonon interactions.[1–3] This is particularly true because of the extreme range of broken-symmetry ground states that are achieved by varying M (Pt, Pd, Ni) and X (Cl, Br, I, etc.) as well as ligands, pressure, magnetic field—ground states ranging from a strongly disproportional CDW (e.g. PtCl) to a weak CDW (e.g. PtI) to SDW or spin-Perierls (and other mixed CDW/SDW[4]) phases (e.g. NiBr, NiCl), in addition to long-period "superlattice" structures.[5]

Theoretically, we have used an Hartree-Fock (H-F) spatially inhomogeneous mean-field approximation (MFA) to study the electronic structure[3] and a direct-space random phase approximation (RPA) to investigate phonons[6] (and associated infrared and Raman spectra) in appropriate many-body Hamiltonians. With parameter input from local-density functional[7] and *ab initio* quantum chemistry calculations,[8] and comparisons with experiments,[1,9] we have employed many-body techniques including H-F, exact diagonalization and adiabatic molecular dynamics to explore the ground and excited states. Agreement between predicted optical, ESR, infrared (IR) and resonance Raman (RR) spectra with recent experiments[1,9,10] on both the pure and mixed-halide MX chains has been quantitatively achieved.

We have modeled effective isolated single chains of pure MX materials in terms of a 3/4-filled, 2-band Peierls extended-Hubbard model. In the case of an isolated mixed-halide chain[11] we replace a segment, containing m X atoms, by X′ atoms where X,X′=Cl, Br, I. Focusing on the metal d_{z^2} and halogen (X,X′) p_x orbitals and including only the nearest neighbor interactions we construct the following tight-binding many-body Hamiltonian:[2,3]

$$
\begin{aligned}
H = \sum_{l,\sigma} \Big\{ & (-t_0 + \alpha\Delta_l)(c^\dagger_{l,\sigma} c_{l+1,\sigma} + c^\dagger_{l+1,\sigma} c_{l,\sigma}) \\
& + [\epsilon_l - \beta_l(\Delta_l + \Delta_{l-1})] c^\dagger_{l,\sigma} c_{l,\sigma} \Big\} + \sum_l U_l n_{l\uparrow} n_{l\downarrow} \\
& + \frac{1}{2} \sum_l K_l \Delta_l^2 + \frac{1}{2} K_{MM} \sum_l (\Delta_{2l} + \Delta_{2l+1})^2 ,
\end{aligned}
\tag{1}
$$

where $c^\dagger_{l,\sigma}(c_{l,\sigma})$ denotes the creation (annihilation) operator for the electronic orbitals at the lth atom with spin σ. M and X (or X′) occupy even and odd sites, respectively. $\Delta_l := \hat{y}_{l+1} - \hat{y}_l$, where $\hat{y}_l$ are the displacements from uniform lattice spacing of the atoms at site l. Equation (1) includes as parameters the onsite energy $\epsilon_l(\epsilon_{2l} = \epsilon_M = e_0; \epsilon_{2l+1} = \epsilon_X = -e_0$ in the X region and $\epsilon_{2l+1} = \epsilon_{X'} = e_0 - 2e'_0$ in the X′ region, ϵ_i being the electron affinity of the ith ion), electron hopping (t_0, t'_0), on-site $(\beta_M, \beta_X, \beta'_X)$ and inter-site (α, α') e-p coupling, on site e-e repulsion (U_m, U_x, U'_X), and finally effective M-X (K) or M-X′ (K′) and M-M (K_{MM}) springs to model the elements of the structure not explicitly included. In particular, (K_{MM}) accounts for the rigidity of the metal sublattice connected into a 3-dimensional network via ligands. Long-range Coulomb fields are also included when necessary - - these effects are especially important for phonon modes around charged excitations (polarons, etc.) in the strongly valence localized cases (e.g. PtCl). Note that the metal M=Pt energies ϵ_{2l} are the same in the segment and the host MX chain. At stoichiometry there are 6 electrons per M_2X_2 (or $M_2X'_2$) unit, or 3/4 band filling. A combination of ground state experimental data (the

X-sublattice distortion amplitude Δ_0, the $\sigma(X) \rightarrow d\sigma^*$ absorption for the oxidized monomer, and the inter-valence charge transfer (IVCT) band edge, E_g, quantum chemical calculations[8] have lead us to the effective parameter sets for the Hamiltonian of Eq. (1).

In the following we present selected results from our comprehensive study for both the pure[3] and mixed-halide[11] MX chains.

Fig. 1 depicts calculated ESR spectra for polarons on a PtBr chain. Fig. 1(a) shows an electron polaron centered on an oxided metal atom ($Pt^{3+\delta}$) while in Fig. 1(b) a hole polaron is centered on a reduced metal atom ($Pt^{3-\delta}$). Since PtBr is a weakly localized CDW system, electron spin density is spread over several sites. Multiple peaks in the ESR spectra are a result of hyperfine splitting due to the interaction between electron and nuclear spin. In the present illustrative calculations we have taken the matrix element for electron-nuclear spin interactions to be the same for both Pt and Br. Note the electron and hole asymmetry in the ESR spectra.

We have also investigated the photodecay channel subsequent to photoexcitation in the ground state as well as in the presence of nonlinear excitations and impurities using adiabatic molecular dynamics.[3]

Next we illustrate a few salient features of *mixed-halide* chains[9,11] by way of predicted optical, infrared (IR) and resonance Raman (RR) spectra. In Fig. 2 a PtCl chain of length N=48 atoms is considered in which a segment containing 8 Cl atoms is replaced by Br atoms. The interface (edge) between the PtCl and PtBr segments is on a reduced metal site ($Pt^{3-\delta}$). Fig. 2 depicts the optical absorption for such a mixed-halide chain. Note that in addition to the two peaks at 1.5 eV and 2.5 eV, which correspond to the inter-valence charge transfer (IVCT) energy for PtBr and PtCl, respectively, there are absorption peaks between the two IVCTs (intragap) as well as several peaks beyond 2.5 eV (ultragap).

We have also identified local *phonon* modes associated with the edge in the mixed-halide chains that correlate directly with the measured RR spectra[9] and the electronic resonance energies of Fig. 2. There are several modes which achieve resonance at energies *between* the IVCT of PtCl and PtBr. The excitation profile for various Raman active modes (not shown) is consistent with the optical absorption shown in Fig. 2.

In conclusion, we have given a brief overview of the important optical

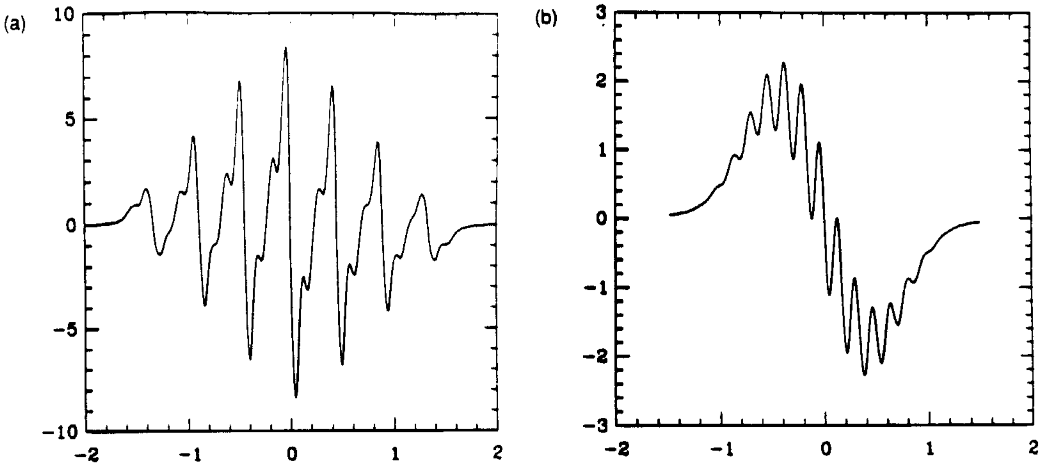

FIGURE 1 The calculated ESR spectrum for (a) an electron polaron and (b) a hole polaron on a PtBr chain.

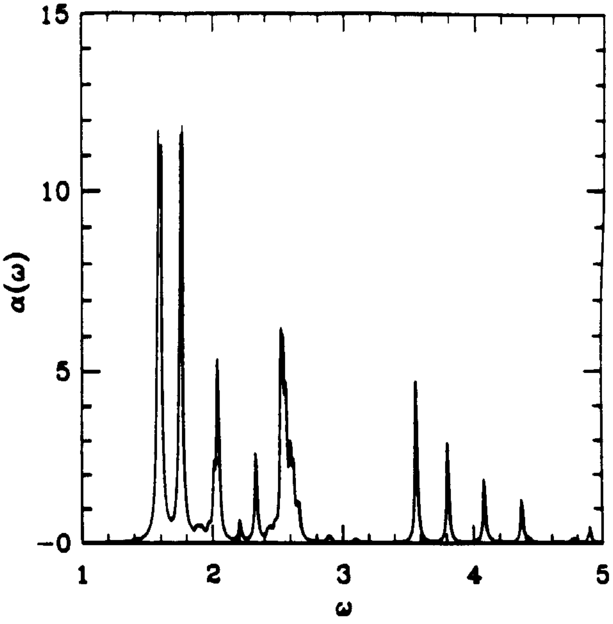

FIGURE 2 Theoretical optical absorption spectra for a mixed-halide chain composed of a segment of 8 Br in a chain of total length 48.

probes in both the pure and mixed-halide MX chain solids. We have also studied the isotope effect in terms of IR and RR signatures of these systems. Furthermore, we are also beginning to explore mixed-metal ($M_xM'_{1-x}X$) and bimetallic (MMX) systems, as well as effects of magnetic fields (especially on the weak CDW/SDW ground state materials[4]). While, we believe that the MX *class* of compounds are nearly uniquely important as a testing ground for many-body modeling and materials design strategy in strongly correlated, low-D materials, we are also on the threshold of investigating their technologically important applications on the other. Indeed, doping and photoexcitation studies of mixed-halide systems[12] indicate that electron and hole defects preferentially locate on differing chain segments (i.e. holes in the PtCl segment, electrons in the PtBr segment). This points to photovoltaic device applications of the mixed-halide single crystals. Similarly, nonlinear optical coefficients on MX films or crystals are beginning to show distinctive properties. Also, since the electronic and spectroscopic properties of MX crystals depend very sensitively on the presence and nature of a variety of impurities, counterions, and ligands, they are very good prospects for chemical sensors.

We acknowledge important discussions with R. Donohoe, X. Z. Huang, B. Swanson and L. Worl. This work was supported by the US DOE.

REFERENCES

1. These proceedings and Proceeding of the ICSM '90, Tübingen, Germany, Synth. Met. **41-43** (1991).
2. J. T. Gammel, R. J. Donohoe, A. R. Bishop and B. I. Swanson, Phys. Rev. B **42**, 10566 (1990).
3. J. T. Gammel, A. Saxena, I. Batistić, A. R. Bishop and S. R. Phillpot, Phys. Rev. B (1991) preprint.
4. H. Röder, J. T. Gammel and A. R. Bishop, preprint.
5. I. Batistić, J. T. Gammel and A. R. Bishop, Phys. Rev. B, preprint.
6. I. Batistić and A. R. Bishop, Phys. Rev. B (1991).
7. R. C. Albers, Synth. Met. **29**, F169 (1989); R. C. Albers, M. Alouani, J. M. Wills and M. Springborg, Synth. Metals **41/3**, 2739 (1991); M. Alouani and R. C. Albers, unpublished.
8. C. Boyle, R. L. Martin and P. J. Hay, unpublished.
9. B. I. Swanson, et al., Synth. Met. **41**, 2733 (1989); Mol. Cryst. Liq. Cryst. **194**, 43 (1991).
10. S. Kurita and M. Haruki, Synth. Met. **29**, F129 (1989); M. Tanaka and S. Kurita, J. Phys. C **19**, 3019 (1986).
11. A. Saxena, X. Z. Huang, I. Batistić, A. R. Bishop, L. A. Worl and B. I. Swanson, Phys. Rev. B, in preparation.
12. L. A. Worl, S. C. Huckett, B. I. Swanson, A. Saxena, A. R. Bishop and J. T. Gammel, Phys. Rev. Lett., preprint.